

# Radial Infall onto a Massive Molecular Filament

Cara Battersby<sup>1</sup>, Philip C. Myers<sup>1</sup>, Yancy L. Shirley<sup>2</sup>, Eric Keto<sup>1</sup>  
and Helen Kirk<sup>3</sup>

<sup>1</sup>Harvard-Smithsonian Center for Astrophysics 60 Garden St., Cambridge, MA 02138 USA  
email: cbattersby@cfa.harvard.edu

<sup>2</sup>Steward Observatory, 933 North Cherry Avenue, Tucson, AZ 85721, USA

<sup>3</sup>Origins Institute, McMaster University, Hamilton, ON, L8S 4M1, Canada

**Abstract.** The newly discovered Massive Molecular Filament (MMF) G32.02+0.05 ( $\sim 70$  pc long,  $10^5 M_{\odot}$ ) has been shaped and compressed by older generations of massive stars. The similarity of this filament in physical structure (density profile, temperature) to much smaller star-forming filaments, suggests that the mechanism to form such filaments may be a universal process. The densest portion of the filament, apparent as an Infrared Dark Cloud (IRDC) shows a range of massive star formation signatures throughout. We investigate the kinematics in this filament and find widespread inverse P cygni asymmetric line profiles. These line asymmetries are interpreted as a signature of large-scale radial collapse. Using line asymmetries observed with optically thick  $\text{HCO}^+$  (1-0) and optically thin  $\text{H}^{13}\text{CO}^+$  (1-0) across a range of massive star forming regions in the filament, we estimate the global radial infall rate of the filament to range from a few 100 to a few 1000  $M_{\odot}\text{Myr}^{-1} \text{pc}^{-1}$ . At its current infall rate the densest portions of the cloud will more than double their current mass within a Myr.

**Keywords.** stars: formation, ISM: kinematics and dynamics

---

## 1. Data and Modelling

We observed 19 pointings toward the highest infrared-extinction region of the G32.02 + 0.05 (G32) Massive Molecular Filament (MMF; see Figure 1) with the Arizona Radio Observatory 12m over 2 nights in March 2013. We used the MAC backend in 2 IF mode with  $0.08 \text{ km s}^{-1}$  resolution to observe the  $\text{HCO}^+$  and  $\text{H}^{13}\text{CO}^+$  (1-0) lines. We used Saturn for main beam calibration, observed in position switching mode, and reduced the data using GILDAS CLASS† software. Our effective spatial resolution is  $\sim 70''$ , or 1.9 pc at the distance of G32 (5.5 kpc; Battersby *et al.* 2014).

We model the spectral line emission by implementing a physical model of the G32 filament based on Herschel data into the radiative transfer code MOLLIE (Keto & Rybicki 2010). We create  $N(\text{H}_2)$  and  $T_{\text{dust}}$  maps of the filament with data from Hi-GAL (Molinari *et al.* 2010) using the methods described in Battersby *et al.* (2011). The average temperature profile across the filament (a cut perpendicular to the long axis of the filament) is relatively flat, with an average  $T_{\text{dust}}$  of 16 K, with a small decrease toward the center of the filament. The average  $N(\text{H}_2)$  profile across the filament can be fit with a Plummer or Gaussian profile. A Plummer profile has the form of  $\rho(r) = \rho_0/[1 + (r/r_{\text{flat}})^2]^{p/2}$  and our best fit value for the inner flat radius,  $r_{\text{flat}}$ , is 0.5 pc and the power-law index,  $p$ , is 2.1. Our best Gaussian fit gave a width (FWHM) of 2.2 pc. *The Plummer profile index is very similar to that found in Arzoumanian et al. (2011), yet our inner flat region is 15 times larger.*

† <http://www.iram.fr/IRAMFR/GILDAS>

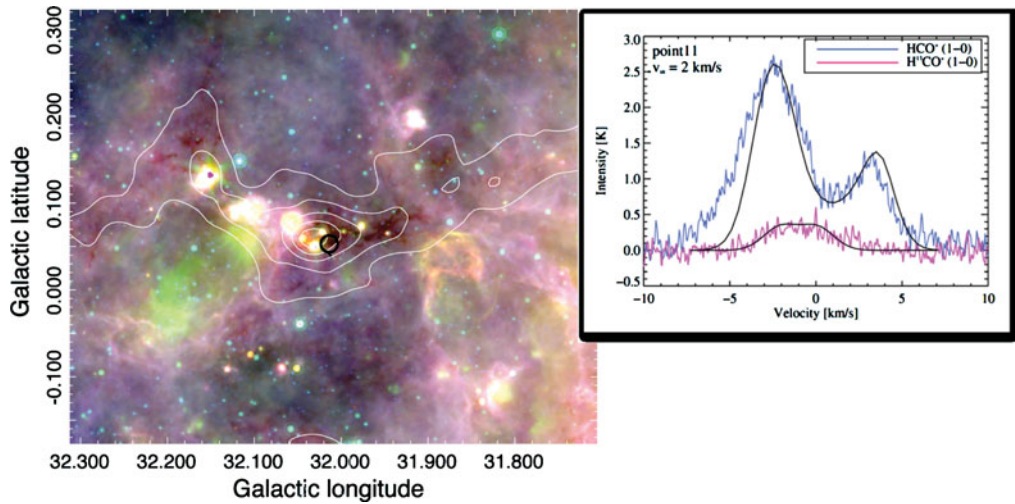


**Figure 1.** The G32.02+0.05 Massive Molecular Filament (MMF) shown on the *left* with 70  $\mu\text{m}$  (Molinari *et al.* 2010) in red, 24  $\mu\text{m}$  (Carey *et al.* 2009) in green, and 8  $\mu\text{m}$  (Benjamin *et al.* 2003) in blue. The white contours show  $^{13}\text{CO}$ -derived column density contours ( $N(\text{H}_2)=0.5\text{--}2.5 \times 10^{22} \text{ cm}^{-2}$ ) from the Galactic Ring Survey (Jackson *et al.* 2006). The filament extends over 70 pc with a total mass of  $\sim 10^5 M_\odot$  (Battersby *et al.* 2014). The spectra on the *right* is  $\text{HCO}^+$  and  $\text{H}^{13}\text{CO}^+$  (1-0) emission from the Arizona Radio Observatory 12m. The black line shows the MOLLIE radiative transfer model spectra for the filament with an infall speed of  $2 \text{ km s}^{-1}$ .

We create a physical model of a cylindrical filament using the average temperature and best-fit Plummer density profile and implement this into the radiative transfer code MOLLIE (Keto & Rybicki 2010). We add a variety of different uniform infall speeds to the physical model and run the radiative transfer code to produce simulated  $\text{HCO}^+$  and  $\text{H}^{13}\text{CO}^+$  (1-0) spectra. We compare these to our observations (see Figure 1) and find that an infall speed of  $2 \text{ km s}^{-1}$  best fits the data.

## 2. Results

We detect widespread infall signatures (inverse P cygni profiles) toward the G32 massive molecular filament. Herschel data show that the G32 filament density profile is well-modeled by a Gaussian or Plummer profile with an index of 2, while the temperature profile is mostly flat with a small dip in the center. We implement a physical model of the filament into a radiative transfer code and find that the inverse P cygni profile is best fit with an infall velocity of  $2 \text{ km s}^{-1}$ . Using a simple equation for the mass flow across a cylindrical surface,  $\dot{M} = \rho\sigma v$ , we find that at a radius of 1 pc, and a variety of reasonable densities from our Herschel fits, an infall speed of  $2 \text{ km s}^{-1}$  corresponds to several 100 to several 1000  $M_\odot \text{ pc}^{-1} \text{ Myr}^{-1}$ . The mass per unit length of the G32 filament varies from several 100 to several 1000  $M_\odot \text{ pc}^{-1}$ , so our infall rates correspond to roughly *doubling the mass of the filament on the timescale of a Myr*.

## References

- Arzoumanian, D., Andre, P., Didelon, P., *et al.* 2011, *A&A*, 529, L6  
 Battersby, C., Bally, J., Ginsburg, A., *et al.* 2011, *A&A*, 535, A128  
 Battersby, C., Ginsburg, A., Bally, J., *et al.* 2014, *ApJ*, 787, 113  
 Benjamin, R. A., Churchwell, E., Babler, B. L., *et al.* 2003, *PASP*, 115, 953

- Carey, S. J., Noriega-Crespo, A., Mizuno, D. R., *et al.* 2009, *PASP*, 121, 76  
Jackson, J. M., Rathborne, J. M., Shah, R. Y., *et al.* 2006, *ApJS*, 163, 145  
Keto, E. & Rybicki, G. 2010, *ApJ*, 716, 1315  
Molinari, S., Swinyard, B., Bally, J., *et al.* 2010, *A&A*, 518, L100  
Molinari, S., Bally, J., Noriega-Crespo, A., *et al.* 2011, *ApJL*, 735, L33